

Sharing Pain: Using Domain Transfer Between Pain Types for Recognition of Sparse Pain Expressions in Horses

Sofia Broomé¹ Katrina Ask³ Maheen Rashid^{4,5} Pia Haubro Andersen³ Hedvig Kjellström^{1,2}
¹ KTH Royal Institute of Technology, Sweden sbroome, hedvig@kth.se ² Silo AI, Sweden
³ Swedish University of Agricultural Sciences katrina.ask, pia.haubro.andersen@slu.se
⁴ University of California, Davis, USA ⁵ Univrses, Sweden maheen.rashid@univrses.com

Abstract

Orthopedic disorders are a common cause for euthanasia among horses, which often could have been avoided with earlier detection. These conditions often create varying degrees of subtle but long-term pain. It is challenging to train a visual pain recognition method with video data depicting such pain, since the resulting pain behavior also is subtle, sparsely appearing, and varying, making it challenging for even an expert human labeler to provide accurate ground-truth for the data. We show that a model trained solely on a dataset of horses with acute nociceptive pain (where labeling is less ambiguous) can aid recognition of the more subtle orthopedic pain. Moreover, we present a human expert baseline for the problem, as well as an extensive empirical study of various domain transfer methods and of what is detected by the pain recognition method trained on acute pain in the orthopedic dataset. Finally, this is accompanied with a discussion around the challenges posed by real-world animal behavior datasets and how best practices can be established for similar fine-grained action recognition tasks. Our code is available at <https://github.com/sofiabroome/painface-recognition>.

1. Introduction

Horses are prey animals of nature, showing as few signs of pain as possible to avoid predators [43]. In domesticated horses, the instinct to hide pain is still present and the presence of humans may disrupt ongoing pain behavior [44]. Recognizing pain can therefore be challenging for both horse owners and equine veterinarian experts, and needs to be improved. An accurate automatic pain detection method has large potential to increase animal welfare.

Orthopedic disorders are frequently seen in horses and are, although treatable if detected early, one of the most common causes for euthanasia [31, 33, 40]. The pain ex-

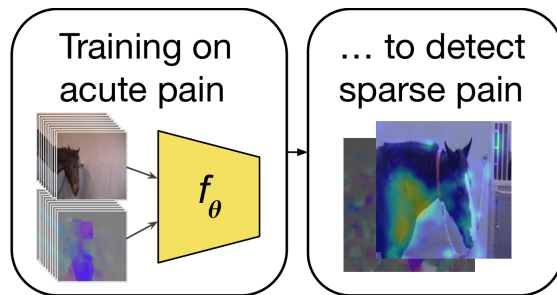


Figure 1: We present a study of domain transfer in the context of different types of pain in horses. Horses under orthopedic pain only show sporadic visual signs of pain, and these signs may overlap with the non-pain class – it is therefore difficult to train a system solely on this data.

perienced by the horse may be low and diffuse, which may leave the injury undetected.

Recognizing horse pain automatically from video requires a method for fine-grained action recognition, which can pick up subtle signals over long time, and is possible to train using a small dataset. In many widely used datasets for action recognition [17, 22, 41], specific objects and scenery may add class information. This is not the case in our scenario, since the only evidence present in the video are the pose, motion and expression of the horse.

The Something-something dataset [27] was indeed collected for fine-grained recognition of action templates, but its action classes are short and atomic. Although the classes in the Diving48 and FineGym datasets [24, 38] are complex and require temporal modeling, the movements that constitute the classes are densely appearing in a sequence during the video, contrary to video data showing horses under orthopedic pain with sparse expressions thereof.

A further important complication is that the labels in the present scenario are inherently noisy since the horse’s subjective experience of pain is not directly observable. Instead, pain induction and/or human pain ratings are used as

proxy when labeling video recordings. To further complicate matters, the behavior patterns that we are searching for might appear in both pain and non-pain data.

Pain assessment in horses is mainly performed by evaluating body behaviors and facial expressions shown by the horse during a short observation period. The observer can either stand outside the box stall or observe the horse in a video. Equine pain research has focused on identifying certain combinations of behaviors and facial expressions for general pain and specific types of pain, such as orthopedic pain [5, 11, 12, 16, 46]. It is important to understand that all behaviors and facial expressions are seen in healthy horses as well, and that the combinations and frequency indicate if pain is present. Being an easier-to-observe special case, recordings of acute pain (applied for short duration and completely reversibly, under ethically controlled conditions) have been used to investigate pain-related facial expressions [15] and for automatic equine pain recognition from video [6]. Until now, it has not been studied how this generalizes to the more clinically relevant orthopedic pain.

This article investigates the automatic recognition of equine orthopedic pain with sparse visual expressions. To tackle the problem, we use domain transfer from the recognition of acute pain, to detect the sparsely appearing visible bursts of pain behavior within orthopedic pain data. We compare the performance of our approach to a human baseline, which we outperform on this specific task (Figure 2).

Our contributions are as follows:

- We are the first to investigate domain transfer between the recognition of different types of pain in animals.
- We present extensive empirical results using two real-world datasets, and highlight challenges arising when moving outside of clean, controlled benchmarking datasets when it comes to computer vision for video.
- We compare domain transfer from a horse pain dataset to standard transferred video features from a general large-scale action recognition dataset, and analyze whether these can complement each other.
- We present an interpretability study of orthopedic pain detection in 25 video clips, firstly for a human expert baseline consisting of 27 equine veterinarians, secondly for one of our neural networks trained to recognize acute pain. We compare what veterinarians typically look for when studying horse pain and what the model finds important for pain classification.

Next, we present related work in Section 2, followed by methodology along with dataset descriptions in Section 3. The emphasis lies on the experiments in Section 4 and discussion thereof, presented in Section 5. Finally, we conclude and outline future directions in Section 6.

2. Related work

Although many methods are relevant to our problem, our setting in terms of data is unique and requires a tailored approach. Weakly supervised action recognition is relevant in that we share the same goal: extracting pertinent information from weakly labeled video data. However, these methods are typically presented under the assumption that there is a large amount of data, which is different from our setting. Our orthopedic pain dataset consists of few (less than 100) and long (in the minutes-range) samples.

Weakly supervised action recognition and localization.

Multiple-instance learning has been used extensively with deep learning for the task of weakly supervised action localization (WSAL), where video level class labels alone are used to determine the temporal extent of class occurrences in videos [21, 34, 30, 29, 47]. However, training deep models within the MIL-scenario can be challenging. The error propagation from the instances may lead to vanishing gradients in MIL [20, 23, 48] and too quick convergence to local optima [10]. This is especially true for the low-sample setting, which is our case.

Typically, videos are split into smaller clips whose predictions are collated to get the video level predictions. Multiple methods use features extracted from a pre-trained two-stream model, I3D [9], as input to their weakly supervised model [21, 30, 34]. In addition to MIL, supervision on feature similarity or difference between clips in videos [21, 30, 51], and adversarial erasing of clip predictions [39, 50] are also used to encourage localization predictions that are temporally complete.

Arnab et al. [4] cast the MIL-problem for video in a probabilistic setting, to tackle its inherent uncertainty. However, they rely on pre-trained recognition of humans in the videos, which aids the action recognition. This is not applicable to our scenario since horses are always present in our frames, and the behaviors we are searching for are more fine-grained than the human actions present in datasets such as [17] or [41] (e.g., fencing or eating). Another difference of WSAL compared to our setting is that we are agnostic as to what types of behavior we are looking for in the videos. For this reason, it is not possible for us to use a localization-by-temporal-alignment method such as the one by [49]. Last, their work relies on a small number of labeled and trimmed instances, which we do not have in this study.

Pain recognition in animals. In [25], an SVM cascade framework is used to recognize facial action units in sheep from single images, to then assess pain according to pre-defined thresholds. A similar method is applied to horses and donkeys in [19], presenting per pain-related facial action unit classification results.

In [32], the work in [25] is continued, using automatically recognized sheep facial landmarks to assess pain on a single-frame basis. In this work, disease progression is monitored from video data, by applying the same pipeline on every 10th frame, and averaging their pain scores. Improving on [25], they use subject-exclusive (leave-one-animal-out) testing for the video part of their experiments.

In a deep learning approach, Tuttle et al. [45] recognize induced inflammatory joint pain in albino mice from single images. While the classification task is binary, the pain labels are set according to human scorings based on facial expressions, on a scale from 1 to 10 (five action units associated with pain that each can have a confidence score of 0-2). It is not clear from the article how they go from the ten-class scale to binary labels. Andresen et al. [3] apply this method to black-furred mice moving more freely in their cages compared to [45], still in a single-frame setting. Both methods [3, 45] use Imagenet [36] pre-trained, standard CNN networks [18, 42] as kept-fixed back-bones, while training a fully-connected classification layer on top of their datasets. Further, both can improve their classification accuracy by averaging the network confidence over images taken within a narrow time span. [3] furthermore point to the difficulty of generalizing between different types of pain, which we investigate closer in this article.

Broomé et al. [6] are the first to perform pain recognition in animals with models learning patterns from sequences rather than single frames, showing large improvement to training on single images. They perform pain recognition using deep recurrent two-stream models, with labels set according to acute induced pain.

3. Method

Central to this study are two datasets depicting pain behavior in horses (Table 1). The datasets are similar in that they both show one horse, trained to stand still, either under pain induction or under baseline conditions (Section 3.1). In our experiments, we investigate the feasibility of knowledge transfer between different pain domains (Section 3.3). We use the macro average F1-score as metric, which is more conservative than accuracy when there is class imbalance.

3.1. Datasets

In Table 1, we show an overview of the two datasets used in this article. It can be noted that neither of the two show a full view of the legs of the horses. This could otherwise be an indicator of orthopedic pain. Both datasets mainly depict the face and upper body of the horses, see, e.g., Figure 3.

3.1.1 The Pain Face dataset (PF)

The experimental setup and video recording of the PF dataset have been described in detail by [6]. Briefly, the

dataset consists of video recordings of six clinically healthy horses with and without acute pain. The pain is either ischemic (from a pressure cuff) or nociceptive (from a chili substance on the skin) and was applied for short durations of time under ethically controlled conditions.

Labels. The induced pain is acute and takes place during a well-defined short time interval, during which the horse shows signs of pain almost continuously. Thus, the video-level label is largely valid for all clips extracted from it.

3.1.2 The EquineOrthoPain(joint) dataset (EOP(j))

The experimental setup for the EOP(j) dataset is thoroughly described in previously published work [5]. Eight clinically healthy horses were recruited for the experiment and acclimatized for 10-12 days prior to induction. During the acclimatization, they were accustomed to standing calmly in the stables, without interacting with their surroundings. Positive reinforcement techniques were used for training.

After the acclimatization, baseline video recordings of each horse standing calmly in the stables were performed. One or two days later, mild to moderate orthopedic pain was induced with lipopolysaccharides (LPS). A diluted ready-made solution was injected into the tarsocrural joint (hock) with routine aseptic techniques. This is a well-known and ethically approved method for orthopedic pain induction in horses and creates a fully reversible acute inflammatory response in the joint, resulting in orthopedic pain.

To follow the progression and regression of pain after induction, several video recordings of 5 minutes were performed during the next 24-48 hours, until each horse was pain-free again. Each video recording was performed with a video camera attached to a tripod at approximately 1.5 metres height and with 1.5 metres distance from the horse.

Labels. In the dataset, there are in total 90 different videos associated with one pain label each (Table 1). Notably, these labels are set before or after the recording of the video. The human raters do not watch the video or the recording of the video. When the labels are set, the horse is still in the box (the recording is made outside of the box), and is being observed by three independent raters. The pain label is the average score of these three ratings. The scores were made using the Composite Pain Scale (CPS) [7], which ranges from 0 to 39. In this study, the lowest pain rating made was 0 and the highest was 10.

For the binary classification used in this study (following prior work [6]), the CPS score is thresholded so that any value larger than zero is labeled as pain, and values equal to zero are labeled as non-pain. This means that we consider even possibly very weak pain signals (e.g., 0.33) as pain for classification, adding to the challenging nature of

	# horses	# videos	# clips	Pain	No pain	Total	Labeling
PF	6	60	8784	03:41:25	06:03:44	09:45:09	Video-level. Induced acute pain, on/off
EOP(j)	7	90	6710	03:37:36	05:03:25	08:41:01	Video-level. Induced orthopedic pain, human CPS pain scoring before/after recording (3 independent raters)

Table 1: Overview of the datasets. Frames are extracted at 2 fps, and clips consist of 10 frames. Duration shown in hh:mm:ss.

the problem. As noted above, the videos for each horse are recorded intermittently during 24-48 hours after the LPS injection, which means that the pain "content" for one subject will vary as the pain progresses and regresses. One of the horses was excluded from our experiments, because it did not have CPS scores > 0 after the pain induction.

3.2. Cross-validation within one domain

When running cross-validation training, we train and test within the same domain. We train with leave-one-subject-out cross-validation. This means that one horse is used as validation set, one horse as held-out test set and the rest of the horses are used as train set. The intention with these experiments is to establish baselines and investigate the treatment of weak labels as dense labels for the two datasets.

Treating weak labels as dense labels. We distinguish between *clips* and *videos*, where clips are five second long windows extracted from the videos (several minutes long). For both datasets, the pain labels have been set weakly on video level. In practice, treating these labels as dense means giving the extracted clips the same label as the video.

Architectures. We use two models in our experiments: the two-stream I3D, pre-trained on Kinetics (kept fixed until Mixed5c), and the recurrent two-stream model (hereon, C-LSTM-2) from [6]. Each stream of C-LSTM-2 consists of four blocks of convolutional LSTM-layers (matrix multiplication in LSTM-equations replaced with convolutions), with max pooling and batch normalization in each. These are fused by addition after the last layer, flattened and input to a two-class classification head. The classification head provided with the I3D implementation is kept and retrained to two classes.

The output of the models are binary pain predictions. We follow the supervised training protocol of [6] with minor modifications, listed in the supplementary material. The main difference is that we resample the minor class clips with a different window stride, to reduce the class imbalance. We also run on a higher frame resolution, 224x224 instead of 128x128. Further implementation details can be found in [6], in the supplementary material and in the public code repository.

3.3. Domain transfer

When running domain transfer experiments, we train a model on the entire dataset from one domain for a fixed number of epochs without validation, and test the trained model on another domain. To choose the number of epochs when training on the entire dataset, we use the average best number of epochs from when running intra-domain cross-validation and multiply this with a factor of how much larger the dataset becomes when including test and validation set (1.5 when going from 4 to 6 horse subjects). This was $77 * 1.5 = 115$ epochs when training C-LSTM on PF, and $42 * 1.5 = 63$ epochs when training I3D on PF. This takes around 80h on a GeForce RTX 2080 Ti GPU for the C-LSTM-2, which is trained from scratch, and around 4h for the I3D where only the classification head is trained. Other than the number of epochs, the model is trained with the same settings as during cross-validation. For I3D, trials with varying numbers of epochs are included in the supplementary material.

3.4. Veterinary expert baseline experiment

As a baseline for orthopedic pain recognition, we engaged 27 Swedish equine veterinarians in rating 25 clips from the EOP(j) dataset. The 25 clips were 5 seconds long, i.e., the same temporal footprint as the inputs to the models.

The clips were sampled from a random point in time from 25 of the videos of the EOP(j) dataset, 13 pain and 12 non-pain. The pain videos were chosen to have a CPS pain label ≥ 1 , in order to have a clearer margin between the two classes, making the task slightly easier than on the entire dataset. Since humans sometimes are present in these videos, correcting the stance of the horses, we first extracted five such clips from random starting points in the video, and used the first of those where the horse was standing reasonably still and without a human occluding it. The veterinarians rated the clips using a 0-10 numerical rating scale (NRS), where 0 corresponded to no pain and 10 to severe pain. The NRS is a commonly used pain assessment tool in humans and seems to be the self-reported scale that correlates best with pain intensity [14]. The participants were carefully instructed that there were clips of horses without and with pain, and that only 0 represented a pain-free state.

Behaviors in the 25 clips (Table 6) were manually iden-

Dataset	# horse folds	F1-score	Accuracy
C-LSTM-2			
PF	6	73.5 \pm 7.1	75.2 \pm 7.4
EOP(j)	7	49.5 \pm 3.6	51.2 \pm 2.8
PF + EOP(j)	13*	60.2 \pm 2.6	61.8 \pm 3.2
(*PF)		69.1 \pm 4.9	71.1 \pm 3.9
(*EOP(j))		53.4 \pm 3.0	53.9 \pm 2.5
I3D			
PF	6	76.1 \pm 1.5	76.6 \pm 1.1
EOP(j)	7	52.2 \pm 2.3	52.6 \pm 2.2
PF + EOP(j)	13*	59.5 \pm 4.3	62.2 \pm 2.7
(*PF)		71.3 \pm 3.5	73.1 \pm 1.4
(*EOP(j))		49.4 \pm 5.3	52.9 \pm 3.7

Table 2: Results (% F1-score) intra-domain cross-validation for the respective datasets and models. The results are averages of five repetitions of a full cross-validation and the average of the per-subject-across-runs standard deviations.

tified and those related to the face were described by two other veterinary experts in consensus according to the Horse Grimace Scale (HGS) [11].

4. Experiments

In this section, we describe our results from intra-domain cross-validation training (4.1), from domain transfer (4.2) and from the human expert baseline study on EOP(j) and its comparison to a model trained on acute pain (4.3).

4.1. Cross-validation within one domain

The results from training with cross-validation within the same dataset are presented in Table 2 for both datasets. When training solely on EOP(j), C-LSTM-2 could not achieve a higher result than random performance (49.5% F1-score), and I3D was just above random (52.2). Aiming to improve the performance, we combined the two datasets in a large 13-fold training rotation scheme. After mixing the datasets, and thereby almost doubling the training set size and number of horses, the total results on 13-fold cross-validation for the two models were 60.2 and 59.5 on average, but where the PF folds on average obtained 69.1 and 71.3 and the EOP(j) folds obtained 53.4 and 49.4. Thus, the performance on PF deteriorated for both models, as well as on EOP(j) for I3D (49.4) and only slightly improved on EOP(j) (53.4) for C-LSTM-2. This indicates that the weak labels of EOP(j) and general domain differences between the datasets hindered standard supervised training with a larger, combined dataset.

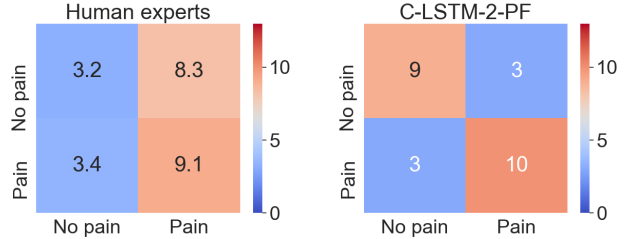


Figure 2: Pain predictions on the 25 clips included in the baseline study (Table 6), by the human experts (left), and by the C-LSTM-2 trained on PF (right).

4.2. Domain transfer to EOP(j)

Table 3 compared to Table 2 shows the importance of domain transfer for the task of recognizing pain in EOP(j). The C-LSTM-2, which has never seen the EOP(j) dataset (hereon, C-LSTM-2-PF), achieves 58.2% F1-score on it – higher than any of the other approaches. I3D, which achieved higher overall score when running cross-validation on PF, did not generalize as well to the unseen EOP(j) dataset (52.7). Fine-tuning these PF-trained instances on EOP(j) decreased the result (54.0 and 51.8, respectively), presumably due to the low signal-to-noise ratio.

Table 4 shows that the results for individual horses may increase when applying a multiple-instance learning filter to the predictions across a video and base the classification only on the top 1%/5% confident predictions (subjects A, H, I, J, K); however, for other subjects, the results decreased (B, N). As described in Section 4.3, there may be large variations among individuals for this type of pain induction.

4.3. Veterinary expert baseline experiment

The method of the expert baseline study is described in Section 3.4. Next, we compare and interpret the decisions of the human experts and the C-LSTM-2-PF.

Comparison between the human experts and the C-LSTM-2-PF. Table 6 is an overview of the ratings given by the experts and the model on the 25 clips. First, we note that the C-LSTM-2-PF instance outperforms the humans on these clips, achieving 76.0% F1-score, compared to 47.6 ± 5.5 for the experts (Figure 2). The experts mainly had difficulties identifying non-pain-sequences. Similarly, when tested on all of EOP(j), the pain F1-score was better than for non-pain for the model instance as well (Table 5), indicating the difficulty of recognizing the non-pain category.

Most of the clips that are rated as painful by the experts contain behaviors that are classically associated with pain, for example in the Horse Grimace Scale [13]. Among the pain clips, clip 6 is the only one without any listed typically pain-related behaviors. The veterinarians score the clip very

Model	A	B	H	I	J	K	N	Global
I3D [9], Kinetics								
PF, EOP(j)-FT	48.7±4.1	56.8±0.9	47.0±3.4	43.6±4.7	53.6±1.7	54.5±0.9	58.2±0.6	51.8±2.3
PF, EOP(j) unseen	54.96	45.05	53.42	56.52	55.69	41.66	46.59	52.70
C-LSTM-2, scratch								
PF, EOP(j)-FT	50.4±2.7	55.1±0.8	44.9±1.4	45.7±0.7	69.3±1.7	51.2 ±0.7	60.8±0.8	54.0±1.3
PF, EOP(j) unseen	61.55	56.34	55.55	51.51	64.76	45.11	57.84	58.17

Table 3: F1-scores on EOP(j), when varying the source of domain transfer, for a model instance trained according to Section 3.3. FT means fine-tuned (three repetitions of full cross-validation runs). Column letters indicate different test subjects.

Model instance	MIL-filter	A	B	H	I	J	K	N
C-LSTM-2-PF	-	61.55	56.34	55.55	51.51	64.76	45.11	57.84
C-LSTM-2-PF	Top 5%	88.31	51.13	59.06	59.06	65.37	31.58	36.36
C-LSTM-2-PF	Top 1%	88.31	51.13	53.33	59.06	65.37	45.83	45.0

Table 4: Results on video-level for EOP(j), when applying a multiple-instance learning (MIL) filter on the clip-level predictions. The column letters designate different test subjects. The model has never trained on EOP(j), and is the same model instance as in Tables 3, 5 and 6.

low (0.96) and seem to agree that the horse does not look painful. The model interestingly scores the clip as painful, but with a very low confidence (0.52).

There are three clips with clear movement of the horse (8, 12, 18), where 8 and 12 are wrongly predicted by the model as being non-pain. Clip 18 is correctly predicted as being non-pain with high confidence (0.9991), suggesting that the model associates movement with non-pain. On clip 18, the human raters mostly agree (17) that this horse does not look painful and the average rating is low (0.96). It can further be noted that the three incorrect pain predictions (17, 20, 24) made by the model occurred when there was either e1 (moderately backwards ears, pointing to the sides) or l (lowered head), or both. Also, 24 is the only clip with a human present, which might have confused the model further (Figure 3).

The four most confident and correct non-pain predictions (>0.99) made by the model are the ones where the head is

Rater	No pain	Pain	Total
Human expert	34.7 ±10.0	60.6 ±4.4	47.6 ±5.5
C-LSTM-2-PF	75.0	76.9	76.0
C-LSTM-2-PF †	54.47	61.86	58.17

Table 5: F1-scores (%) on the 25 clips of the expert baseline. The C-LSTM-2-PF instance was trained on PF but never on EOP(j). †-symbol: results on the entire EOP(j) dataset for comparison.

held in a clear, upright (u) position. Similarly, the three most confident and correct pain predictions (>0.99) by the model all contain ear behavior (e1 or e2).

Why is the expert performance so low? Tables 5, 7 and Figure 2 show a low performance for the human experts in general and especially for non-pain.

Increasing the threshold to 1 and 2 reduced the accuracy for pain, which may be due to false inclusion of scores of 0 if the raters scored 1 or 2 for non-pain, contrary to the instructions. Vice versa, the accuracy for non-pain increased when threshold was extended, which may be due to inclusion of scores of 1 and 2, used as non-pain (even though they were informed that only 0 is used for non-pain).

The results point to the difficulty of observing pain expressions at a random point in time for orthopedic pain, and without context. The LPS-induced orthopedic pain may further have complicated the rating process, since it often varies in intensity among individuals, despite administration of the same dose. This results in different levels of pain expressions [2], sometimes occurring intermittently. Hence, there will be 'windows' during the observed time where the horse expresses pain clearly [35]. The other parts of the observed time will then contain combinations of facial expressions that some raters interpret as non-pain, and some raters interpret as pain. If a 'window' is not included in the 5 second clip, it is difficult for the rater to assign a score, decreasing their accuracy.

Clip	Behaviors	CPS	Label	27 Experts		C-LSTM-2-PF	
				Avg. rating	# correct	Pred.	Conf.
1	e1	2	1	2.7	23	1	0.9999
2	o1 l	2	1	1.1	10	1	0.9241
3	e2 t1 c1 n1 p	4.33	1	3.4	22	1	0.9997
4	e2 o1 l	4.67	1	3.7	21	1	0.6036
5	t1 c1	3.67	1	0.37	4	1	0.9853
6		1.33	1	0.96	13	1	0.5200
7	u	4.33	1	1.3	12	1	0.9063
8	c2 n2 m u p	6.33	1	4.7	25	0	0.8623
9	e1 t1 c1 n1 p	3	1	4.6	25	0	0.5504
10	e2 t1 c1 n2 l p	2	1	4.4	25	1	0.9999
11	e2 t1 c1 n2 l	1	1	6.8	27	1	0.8231
12	e1 t1 c1 n1 m	4.33	1	2.5	22	0	0.8046
13	e2 t1 c1 n2	1.67	1	4.4	26	1	0.9840
14	e2 o1 t1 c1 n1 u	0	0	5.5	0	0	0.9993
15	e2 t1	0	0	4.1	1	0	0.5848
16	e2 o1 t1 c1 n1	0	0	3.9	4	0	0.8439
17	e1 o1 t1 n1 l p	0	0	4.4	5	1	0.6456
18	t1 m u p	0	0	0.96	17	0	0.9991
19		0	0	0.48	21	0	0.9568
20	t1 l	0	0	2.9	9	1	1.00
21	u	0	0	1.3	13	0	0.9999
22		0	0	2.7	4	0	0.6128
23	c1 n1 u	0	0	1.6	8	0	0.9989
24	e1 t1 n1 h p	0	0	2.4	9	1	1.00
25	e2 o1 t1 n1	0	0	5.9	0	0	0.6135

Table 6: Overview of the predictions on 25 EOP(j) clips made by the human veterinarian experts and by the C-LSTM-2, trained only on PF. The labels for the C-LSTM-2 were thresholded above 0 (same threshold as for the experts).

5. Discussion

The human expert baseline for classification on clip-level of the EOP(j) dataset, which was on average 51.3% accurate, together with Table 2 indicates the level of difficulty in detecting orthopedic pain during short observation.

Labels in the real world. None of the equine pain datasets were recorded with the intention to run machine learning on the videos. This presents noise, in both data and labels.

Threshold	No pain	Pain	Total
0	28.1 \pm 11.2	72.7 \pm 9.4	51.3 \pm 4.6
1	37.4 \pm 14.1	65.2 \pm 9.7	51.9 \pm 5.7
2	48.5 \pm 18.7	52.7 \pm 13.8	50.7 \pm 7.5

Table 7: Accuracies (%) from the expert baseline, varying with the chosen pain threshold.

Weakly supervised training on EOP(j). During the course of this study, we performed a large number of experiments in a weakly supervised training regime on EOP(j). Our approach was to extract features from pre-trained networks and combine these into full video-length, to then run multiple-instance learning training on the feature sequences (the assumption being that a pain video would contain many negative instances as well). Training on the full video-length is computationally feasible since the features are low-dimensional compared to the raw video input. The predictions from the pre-trained networks were also used in this training scheme, both as attention within a video-level model or as pseudo-labels when computing the various loss functions we experimented with. The results were unsatisfactory, and were not higher than the C-LSTM-2-PF tested on the unseen EOP(j) data, even when re-using the features from that same model instance. Our main obstacle, we hypothesize, was the low statistical sample size (90) on video-level. To run weakly supervised action or behavior recognition, a large number of samples, simply a lot of data, is needed – otherwise the training is not stable. This was vis-

Figure 3: **The figures can be displayed on click as videos in Adobe Reader.** RGB (left), optical flow (middle), and Grad-CAM [37] saliency maps (right) of the C-LSTM-2-PF predictions on clips 10 and 24 (Table 6). Clip 10 (top) is a correct prediction of pain. The bottom row is a failure case, showing an incorrect pain prediction, and we observe that the model partly focuses on the human bystander. The remaining 23 clips with saliency maps can be found in the supplementary.

ible from the significant variance across repeated runs in this type of setting. Controlled video data of the same horse subjects, in pain and not, does not (and, arguably, should not) exist in abundance. For this reason, we resorted to domain transfer from acute pain as the better option for our conditions.

Domain transfer: Why does the C-LSTM-2 generalize better than I3D? Despite performing better on PF during intra-domain cross-validation than the C-LSTM-2, I3D does worse upon domain transfer to a new dataset (Table 3). It is furthermore visible in Table 2 that the I3D performance on EOP(j) deteriorates when combining the two datasets, perhaps indicating a proneness to learning dataset-specific spurious correlations which do not combine well. In contrast, the C-LSTM-2 slightly improves its performance on EOP(j) when merging the two training sets.

We hypothesize that this is because I3D is an over-parameterized model (25M parameters), compared to the C-LSTM-2 (1.5M parameters). An I3D pre-trained on Kinetics with its large number of trainable parameters is excellent when a model needs to memorize many, predominantly spatial, features of a large-scale dataset with cleanly separated classes, in an efficient way. When it comes to fine-grained classification of a lower number of classes, which can generalize to a slightly different domain, and moreover requires more temporal modeling than when the task is to separate 'playing trumpet' from 'playing violin' (or at Kinetics' most challenging: 'dribbling' from 'dunking'), it seems, from our experiments, that it is not a suitable archi-

itecture.

Another reason could be the fact that the C-LSTM-2 is trained solely on horse data, from the bottom up, while the I3D has its back-bone unchanged in our experiments. In that light, the C-LSTM-2 can be considered more specialized to the problem. Although Kinetics-400 does contain two classes related to horses: 'grooming horse' and 'riding or walking with horse', the C-LSTM-2 undoubtedly has seen more up-close footage of horses. In fact, somewhat ironically, the 'riding or walking with horse' coupled with 'riding mule' is listed in [22] as the top confused class of the dataset, using the two-stream I3D. So how would I3D do if trained solely on the PF dataset? This is where the model size becomes a problem. I3D requires large amounts of training data to converge properly; the duration of Kinetics-400 is around 450h. It is for ethical reasons difficult to collect a 450h video dataset (>40 times larger than PF) with controlled pain labels.

6. Conclusions

We have shown that domain transfer is possible between different pain types in horses. This was achieved through experiments on two real-world datasets presenting significant challenges from noisy labels, low number of samples and subtle distinction in behavior between the two classes. We furthermore described the challenges arising when attempting to move out of the cleaner bench-marking dataset realm, which is still under-explored in action recognition. Our study indicated that a deep state-of-the-art model pre-trained on Kinetics was not necessarily suited for fine-grained action classification of this kind. A comparison between 27 equine veterinarians and a neural network trained on acute pain was conducted on which behaviors were preferred by the two, respectively. The comparison indicated that the neural network prioritized other behaviors than humans during pain-non-pain classification.

We presented the first attempt at recognizing orthopedic pain from raw video data and hope that our work can serve as a stepping stone toward further recognition and analysis of horse pain behavior in video.

6.1. Future work

Directions for future work include processing data showing the horse in a more natural environment, such as its box or outdoors, amidst the flock, though it might be challenging to collect data in these circumstances. This would require a more robust tracking of the horse in the video, for instance using animal pose estimation methods such as [8, 28]. Learning to separate stress from pain is another important but difficult avenue to consider [26, 1].

References

- [1] Pia Haubro Andersen, Sofia Broomé, Maheen Rashid, Johan Lundblad, Katrina Ask, Zhenghong Li, Elin Hernlund, Marie Rhodin, and Hedvig Kjellström. Towards machine recognition of facial expressions of pain in horses. *Animals*, 11(6), 1643, 2021. [8](#)
- [2] S. M. Andreassen, A. M. L. Vinther, S. S. Nielsen, P. H. Andersen, A. Tnibar, A. T. Kristensen, and S. Jacobsen. Changes in concentrations of haemostatic and inflammatory biomarkers in synovial fluid after intra-articular injection of lipopolysaccharide in horses. *BMC Veterinary Research*, 13(1):182, 2017. [6](#)
- [3] Niek Andresen, Manuel Wöllhaf, Katharina Hohlbaum, Lars Lewejohann, Olaf Hellwich, Christa Thöne-Reineke, and Vitaly Belik. Towards a fully automated surveillance of well-being status in laboratory mice using deep learning: Starting with facial expression analysis. *PLOS ONE*, 15(4):1–23, 04 2020. [3](#)
- [4] Anurag Arnab, Chen Sun, Arsha Nagrani, and Cordelia Schmid. Uncertainty-aware weakly supervised action detection from untrimmed videos. In Andrea Vedaldi, Horst Bischof, Thomas Brox, and Jan-Michael Frahm, editors, *Computer Vision – ECCV 2020*, pages 751–768, Cham, 2020. Springer International Publishing. [2](#)
- [5] Katrina Ask, Marie Rhodin, Lena-Mari Tamminen, Elin Hernlund, and Pia Haubro Andersen. Identification of body behaviors and facial expressions associated with induced orthopedic pain in four equine pain scales. *Animals*, 10(11), 2020. [2](#), [3](#)
- [6] Sofia Broomé, Karina Bech Glerup, Pia Haubro Andersen, and Hedvig Kjellström. Dynamics are important for the recognition of equine pain in video. In *The IEEE Conference on Computer Vision and Pattern Recognition (CVPR)*, June 2019. [2](#), [3](#), [4](#), [11](#), [12](#)
- [7] G. Bussi eres, C. Jacques, O. Lainay, G. Beauchamp, A. Leblond, J.L. Cador e, L.M. Desmaizi eres, S.G. Cuvelliez, and E. Troncy. Development of a composite orthopaedic pain scale in horses. *Res Vet Sci*, 85(2), 2008. [3](#)
- [8] Jinkun Cao, Hongyang Tang, Hao-Shu Fang, Xiaoyong Shen, Cewu Lu, and Yu-Wing Tai. Cross-domain adaptation for animal pose estimation. In *Proceedings of the IEEE/CVF International Conference on Computer Vision (ICCV)*, October 2019. [8](#)
- [9] Joao Carreira and Andrew Zisserman. Quo Vadis, Action Recognition? A New Model and the Kinetics Dataset. In *CVPR*, 2017. [2](#), [6](#), [14](#)
- [10] Ramazan Gokberk Cinbis, Jakob Verbeek, and Cordelia Schmid. Weakly Supervised Object Localization with Multi-Fold Multiple Instance Learning. *IEEE Transactions on Pattern Analysis and Machine Intelligence*, 39(1):189–203, 2017. [2](#)
- [11] E. Dalla Costa, M. Minero, D. Lebelt, D. Stucke, E. Canali, and M. C. Leach. Development of the Horse Grimace Scale (HGS) as a Pain Assessment Tool in Horses Undergoing Routine Castration. *PLoS ONE*, 9(3), 2014. [2](#), [5](#), [11](#)
- [12] E. Dalla Costa, D. Stucke, F. Dai, M. Minero, M. C. Leach, and D. Lebelt. Using the horse grimace scale (HGS) to assess pain associated with acute laminitis in horses (*Equus caballus*). *Animals*, 6(47):1–9, 2016. [2](#)
- [13] de Camp Nora V., Ladwig-Wiegard Mechthild, Geitner Carolina I.E, and Bergeler J urgen nad Th one-Reineke Christa. Eeg based assessment of stress in horses: A pilot study. *PeerJ*, 8:e8629:1–15, 2020. [5](#)
- [14] M. A. Ferreira-Valente, J. L. Pais-Ribeiro, and M. P. Jensen. Validity of four pain intensity rating scales. *Pain*, 152(10):2399–2404, oct 2011. [4](#)
- [15] K. B. Glerup, B. Forkman, C. Lindegaard, and P. H. Andersen. An equine pain face. *Veterinary Anaesthesia and Analgesia*, 42, 2015. [2](#)
- [16] K. B. Glerup and C. Lindegaard. Recognition and quantification of pain in horses: A tutorial review. *Equine Veterinary Education*, 28(1):47–57, 2016. [2](#)
- [17] Chunhui Gu, Chen Sun, David A. Ross, Carl Vondrick, Caroline Pantofaru, Yeqing Li, Sudheendra Vijayanarasimhan, George Toderici, Susanna Ricco, Rahul Sukthankar, Cordelia Schmid, and Jitendra Malik. Ava: A video dataset of spatio-temporally localized atomic visual actions. In *Proceedings of the IEEE Conference on Computer Vision and Pattern Recognition (CVPR)*, June 2018. [1](#), [2](#)
- [18] K. He, X. Zhang, S. Ren, and J. Sun. Deep residual learning for image recognition. In *2016 IEEE Conference on Computer Vision and Pattern Recognition (CVPR)*, pages 770–778, 2016. [3](#)
- [19] H. I. Hummel, F. Pessanha, A. Salah, T. M. van Loon, and R. C. Veltkamp. Automatic pain detection on horse and donkey faces. In *2020 15th IEEE International Conference on Automatic Face and Gesture Recognition (FG 2020) (FG)*, pages 717–724, Los Alamitos, CA, USA, may 2020. IEEE Computer Society. [2](#)
- [20] Maximilian Ilse, Jakub M Tomczak, and Max Welling. Attention-based deep multiple instance learning. *arXiv preprint arXiv:1802.04712*, 2018. [2](#)
- [21] Ashraf Islam and Richard Radke. Weakly supervised temporal action localization using deep metric learning. In *Proceedings of the IEEE/CVF Winter Conference on Applications of Computer Vision (WACV)*, March 2020. [2](#)
- [22] Will Kay, Jo ao Carreira, Karen Simonyan, Brian Zhang, Chloe Hillier, Sudheendra Vijayanarasimhan, Fabio Viola, Tim Green, Trevor Back, Paul Natsev, Mustafa Suleyman, and Andrew Zisserman. The kinetics human action video dataset. *CoRR*, abs/1705.06950, 2017. [1](#), [8](#)
- [23] Xiaodan Li, Yining Lang, Yuefeng Chen, Xiaofeng Mao, Yuan He, Shuhui Wang, Hui Xue, and Quan Lu. Sharp multiple instance learning for deepfake video detection. *Proceedings of the 28th ACM International Conference on Multimedia*, Oct 2020. [2](#)
- [24] Yingwei Li, Yi Li, and Nuno Vasconcelos. Resound: Towards action recognition without representation bias. In *Proceedings of the European Conference on Computer Vision (ECCV)*, September 2018. [1](#)
- [25] Y. Lu, M. Mahmoud, and P. Robinson. Estimating Sheep Pain Level Using Facial Action Unit Detection. In *12th IEEE International Conference on Automatic Face & Gesture Recognition (FG 2017)*, 2017. [2](#), [3](#)

- [26] Johan Lundblad, Maheen Rashid, Marie Rhodin, and Pia Haubro Andersen. Effect of transportation and social isolation on facial expressions of healthy horses. *PLoS One*, 16(6), 2021. **8**
- [27] Farzaneh Mahdisoltani, Guillaume Berger, Waseem Gharbieh, David J. Fleet, and Roland Memisevic. Fine-grained video classification and captioning. *CoRR*, abs/1804.09235, 2018. **1**
- [28] Alexander Mathis, Thomas Biasi, Steffen Schneider, Mert Yuksekgonul, Byron Rogers, Matthias Bethge, and Mackenzie W. Mathis. Pretraining boosts out-of-domain robustness for pose estimation. In *Proceedings of the IEEE/CVF Winter Conference on Applications of Computer Vision (WACV)*, pages 1859–1868, January 2021. **8**
- [29] Phuc Nguyen, Ting Liu, Gautam Prasad, and Bohyung Han. Weakly supervised action localization by sparse temporal pooling network. In *CVPR*, 2018. **2**
- [30] Sujoy Paul, Sourya Roy, and Amit K Roy-Chowdhury. W-TALC: Weakly-supervised Temporal Activity Localization and Classification. In *Proceedings of the European Conference on Computer Vision (ECCV)*, pages 563–579, 2018. **2**
- [31] J. C. Penell, A. Egenvall, B. N. Bonnett, P. Olson, and J. Pringle. Morbidity of Swedish horses insured for veterinary care between 1997 and 2000: variations with age, sex, breed and location. *Veterinary Record*, 157:470–477, 2000. **1**
- [32] P. Pessanha, K. McLennan, and M. Mahmoud. Towards automatic monitoring of disease progression in sheep: A hierarchical model for sheep facial expressions analysis from video. In *15th IEEE International Conference on Automatic Face & Gesture Recognition (FG 2020)*, 2020. **3**
- [33] D. Pollard, C. E. Wylie, J. R. Newton, and K. L.P. Verheyen. Factors associated with euthanasia in horses and ponies enrolled in a laminitis cohort study in Great Britain. *Preventive Veterinary Medicine*, 174(November 2019):104833, 2020. **1**
- [34] Maheen Rashid, Hedvig Kjellström, and Yong Jae Lee. Action graphs: Weakly-supervised action localization with graph convolution networks. In *The IEEE Winter Conference on Applications of Computer Vision*, pages 615–624, 2020. **2**
- [35] Maheen Rashid, Alina Silventoinen, Karina Bech Gleerup, and Pia Haubro Andersen. Equine facial action coding system for determination of pain-related facial responses in videos of horses. *PLOS ONE*, 15(11):1–18, 11 2020. **6**
- [36] Olga Russakovsky, Jia Deng, Hao Su, Jonathan Krause, Sanjeev Satheesh, Sean Ma, Zhiheng Huang, Andrej Karpathy, Aditya Khosla, Michael Bernstein, Alexander C. Berg, and Li Fei-Fei. ImageNet Large Scale Visual Recognition Challenge. *International Journal of Computer Vision (IJCV)*, 115(3):211–252, 2015. **3**
- [37] Ramprasaath R. Selvaraju, Michael Cogswell, Abhishek Das, Ramakrishna Vedantam, Devi Parikh, and Dhruv Batra. Grad-CAM: Visual Explanations from Deep Networks via Gradient-Based Localization. *Proceedings of the IEEE International Conference on Computer Vision*, 2017-Octob:618–626, 2017. **8, 11, 12, 13**
- [38] Dian Shao, Yue Zhao, Bo Dai, and Dahua Lin. Finegym: A hierarchical video dataset for fine-grained action understanding. In *IEEE Conference on Computer Vision and Pattern Recognition (CVPR)*, 2020. **1**
- [39] Krishna Kumar Singh and Yong Jae Lee. Hide-and-seek: Forcing a network to be meticulous for weakly-supervised object and action localization. In *ICCV*, 2017. **2**
- [40] J. Slayter and G. Taylor. National Equine Health Survey (NEHS) 2018. Technical report, 2018. **1**
- [41] Khurram Soomro, Amir Roshan Zamir, and Mubarak Shah. Ucf101: A dataset of 101 human actions classes from videos in the wild. *CoRR*, abs/1212.0402, 2012. **1, 2**
- [42] Christian Szegedy, Vincent Vanhoucke, Sergey Ioffe, Jonathon Shlens, and Zbigniew Wojna. Rethinking the inception architecture for computer vision. In *Proceedings of IEEE Conference on Computer Vision and Pattern Recognition*, 2016. **3**
- [43] P. M. Taylor, P. J. Pascoe, and K. R. Mama. Diagnosing and treating pain in the horse. Where are we today? *Veterinary Clinics of North America - Equine Practice*, 18(1):1–19, 2002. **1**
- [44] Catherine Torcivia and Sue McDonnell. In-person caretaker visits disrupt ongoing discomfort behavior in hospitalized equine orthopedic surgical patients. *Animals*, 10(2), 2020. **1**
- [45] Alexander H Tuttle, Mark J Molinaro, Jasmine F Jethwa, Susana G Sotocinal, Juan C Prieto, Martin A Styner, Jeffrey S Mogil, and Mark J Zylka. A deep neural network to assess spontaneous pain from mouse facial expressions. *Molecular Pain*, 14:1744806918763658, 2018. PMID: 29546805. **3**
- [46] J. P. A. M. van Loon and M. C. Van Dierendonck. Objective pain assessment in horses (2014–2018). *Veterinary Journal*, 242:1–7, 2018. **2**
- [47] Limin Wang, Yuanjun Xiong, Dahua Lin, and Luc Van Gool. Untrimmednets for weakly supervised action recognition and detection. In *CVPR*, 2017. **2**
- [48] Xinggong Wang, Yongluan Yan, Peng Tang, Xiang Bai, and Wenyu Liu. Revisiting multiple instance neural networks. *arXiv preprint arXiv:1610.02501*, 2016. **2**
- [49] Pengwan Yang, Vincent Tao Hu, Pascal Mettes, and Cees G. M. Snoek. Localizing the common action among a few videos. In Andrea Vedaldi, Horst Bischof, Thomas Brox, and Jan-Michael Frahm, editors, *Computer Vision – ECCV 2020*, pages 505–521, Cham, 2020. Springer International Publishing. **2**
- [50] Runhao Zeng, Chuang Gan, Peihao Chen, Wenbing Huang, Qingyao Wu, and Mingkui Tan. Breaking winner-takes-all: Iterative-winners-out networks for weakly supervised temporal action localization. *IEEE Transactions on Image Processing*, 2019. **2**
- [51] Yuanhao Zhai, Le Wang, Ziyi Liu, Qilin Zhang, Gang Hua, and Nanning Zheng. Action coherence network for weakly supervised temporal action localization. In *ICIP*, 2019. **2**

A. Supplementary material for the human expert study

Table 8 lists the different behavior symbols which appear in Table 6 of the main article.

Behavior	Symbol
<i>From the Horse Grimace Scale [11]</i>	
Backwards ears, moderately present	e1
Backwards ears, obviously present	e2
Orbital tightening, moderately present	o1
Orbital tightening, obviously present	o2
Tension above the eye area, moderately present	t1
Tension above the eye area, obviously present	t2
Mouth strained and pronounced chin, moderately present	c1
Mouth strained and pronounced chin, obviously present	c2
Strained nostrils and flattening of the profile, moderately present	n1
Strained nostrils and flattening of the profile, obviously present	n2
<i>Other</i>	
Large movement	m
Mouth play	p
Lowered head	l
Clearly upright head	u
Human in clip	h

Table 8: Symbols accompanying Table 4 in the main article.

In Figures 4-5, we show RGB, optical flow and Grad-CAM [37] saliency maps for each of the classification decisions on clip 1-25 taken by C-LSTM-2-PF. The clips are the same as the ones listed in Table 6 of the main article.

B. Supplementary experiments

B.1. Domain transfer results for additional model instances

Table 9 contains results for repeated runs of training C-LSTM-2 on the entire PF dataset for 115 epochs. Importantly, it contains further results on I3D trained on the entire PF dataset for a varied number of epochs. This is to make sure that we did not miss out on better performing behavior of I3D in our comparison.

The reason for the slight discrepancy between the global F1-scores and the subject-wise F1-scores is due to the varying proportions of pain and non-pain clips between the subjects. In the global setting, the classes are approximately

balanced due to the resampling procedure (Section C.1.1). Since the F1-score is the harmonic mean of precision and recall, a non-linear function, it does not simply behave as a mean when it is computed for different parts of a training set.

B.2. Cross-validation within one domain on smaller frames

Table 10 shows cross-validated intra-domain results for C-LSTM-2 when the input resolution is 128x128 pixels. This is the same input resolution as in [6], but the training was conducted along with the training modifications listed in Section C.1 (except for the frame resolution). The observation that treating weak labels as dense labels works for acute pain (PF) but not for orthopedic pain (EOP(j)), where the expressions are sparse over time, still holds for input data of this size.

C. Training details

C.1. Modified training of the C-LSTM-2 [6]

We follow the supervised training protocol of [6] but make the following modifications.

- We run on 224x224x3 frames, instead of 128x128x3. This forces us to use a batch size of 2 instead of 8 on a GPU with 11GB memory (the sequence length is kept at 10). However, Table 10 shows cross-validation results for C-LSTM-2 on 128x128 resolution on the two datasets (batch size 8).
- Each clip is horizontally flipped with 0.5 probability, as data augmentation.
- Clip-level binary cross-entropy is used during optimization, instead of on frame-level as in [6]. The test results in [6] were presented as majority votes across clips. Here, we use clip-level classifications during both training, validation and testing.
- The RGB data is standardized according to the pixel mean and standard deviation of the dataset. The optical flow data in the two-stream model is linearly scaled to the 0-1 range from the 0-255 jpg range, to have similar magnitude as the RGB data.
- Since there is class imbalance, we resample the minor class (i.e., we extract sequences more frequently across a video, details in Section C.1.1). This is done during validation and testing as well, for easier interpretation of the results.
- We train for maximum 200 epochs, with 50 epochs early stopping based on the validation set, and use the model state at the epoch with best performance on the



Figure 4: Every pain-clip from the human expert baseline (clips 1-13). **The figures can be displayed on click as videos in Adobe Reader.** RGB (left), optical flow (middle), and Grad-CAM [37] saliency maps (right) of the C-LSTM-2-PF predictions on clips 1-13 (Table 6 in the main article).

validation set to run on the held-out test subject. In [6], the maximum number of epochs was 100, with 15 epochs early stopping.

C.1.1 Algorithm for clip resampling

Clip resampling of the minor class (typically the pain class) was introduced to have class balance. Frames from the videos are extracted at 2fps. The clips consist of windows

14	15
16	17
18	19
20	21
22	23
24	25

Figure 5: Every non-pain-clip from the human expert baseline (clips 14-25). **The figures can be displayed on click as videos in Adobe Reader.** RGB (left), optical flow (middle), and Grad-CAM [37] saliency maps (right) of the C-LSTM-2-PF predictions on clips 14-25 (Table 6 in the main article).

of frames with a certain window length w_L , extracted with some window stride w_S , across a video. Before resampling, $w_L = 10$ and $w_S = 10$ (back-to-back window extraction), and the start index for extraction $t_{start} = 0$. When resampling, in order to obtain a number of clips from the same video which are maximally different from the previously extracted clips, we want to sample starting from the index $t_{start} = \frac{w_L}{2}$, which in this case equals five.

For each training/validation/test split, we sample as many clips as required to have an equal number of pain and non-pain clips: $n_{resample} = \text{abs}(n_{minor class} -$

$n_{major class})$. We resample $n_{resample}/M$ clips per video, where M is the total number of videos of a dataset. The code used for the resampling can be found in the public repository.

M, E	A	B	H	I	J	K	N	Global
I3D [9], Kinetics								
PF †, 63	54.96	45.05	53.42	56.52	55.69	41.66	46.59	52.70
PF, 25	51.0 ±0.9	46.7 ±0.63	45.5 ±7.33	52.1 ±1.8	56.0 ±4.23	41.5 ±0.43	46.2 ±2.4	51.7 ±1.4
PF, 63	49.9 ±2.8	48.0 ±2.1	47.2 ±2.6	52.2 ±1.8	59.0 ±1.0	40.7 ±0.8	46.1 ±2.2	52.6 ±0.4
PF, 115	49.8 ±1.8	48.1 ±1.5	45.1 ±1.8	54.0 ±0.8	58.9 ±1.3	40.2 ±0.8	47.0 ±1.1	52.6 ±0.05
PF, 200	50.2 ±2.2	46.9 ±0.9	50.2 ±1.8	51.1 ±1.4	58.5 ±0.6	41.3 ±0.2	47.1 ±1.4	52.4 ±0.5
C-LSTM-2, scratch								
PF †, 115	61.55	56.34	55.55	51.51	64.76	45.11	57.84	58.17
PF, 115	59.4 ±4.6	56.7 ±2.7	60.5 ±5.7	52.1 ±1.8	53.2 ±14.0	49.6 ±3.9	54.2 ±4.2	56.3 ±2.8

Table 9: M for model, E for epochs, A, B, H, I, J, K, N for different horse subjects, † for the instance used in the main article. Repetitions (three repetitions whenever a mean and standard deviation are presented) of the results in Table 3 of the main article, and supplementary runs for I3D for a varying number of epochs.

Dataset	Horse folds	F1-score	Accuracy
PF	6	80.7 ±4.4	81.2 ±3.9
EOP(j)	7	48.3 ±3.6	49.4 ±3.2
PF + EOP(j)*	13	58.5 ±4.5	60.3 ±4.1
(*PF)		70.8 ±4.1	73.0 ±4.1
(*EOP(j))		48.0 ±4.8	49.3 ±4.2

Table 10: Results (%) on 128x128 frames from training on clip-level for the respective datasets using the C-LSTM-2. The total result is the average of five repetitions of a full cross-validation and the average of the per-subject-across-runs standard deviations.